

Thermal Diffusivity of Lherzolite at High Pressures and High Temperatures Using Pulse Method

Sheqiang Miao¹, Yongsheng Zhou¹, Heping Li²

1. State Key Laboratory of Earthquake Dynamics, Institute of geology, China Earthquake Administration, Beijing 100029, China

2. CAS Key Laboratory of High-Temperature and High-Pressure Study of the Earth's Interior, Institute of Geochemistry, Chinese Academy of Sciences, Guiyang 550081, China.

Sheqiang Miao: <https://orcid.org/0000-0002-2240-1580>

ABSTRACT: Lherzolite is one of the most important components of the subcontinental mantle lithosphere, and the study of its heat transfer properties aids in understanding the thermal structure of the continental mantle lithosphere. Currently, few studies have examined the heat transfer properties of lherzolite, and the experimental results remain controversial. This experiment utilized a pulse method to measure the thermal diffusivity of lherzolite at pressures ranging from 1.0 to 4.0 GPa and temperatures from 300 to 1 073 K on a cubic press apparatus. We obtained a thermal diffusivity for lherzolite of approximately $2.10 \text{ mm}^2\text{s}^{-1}$ at ambient condition. The experimental pressure derivative of the thermal conductivity of lherzolite decreased with temperature, reaching approximately 10% at high temperature, a value higher than the previously reported 4%, which indicates that the temperature gradient of the upper mantle lithosphere is smaller than previously thought. Therefore, concerning calculation of the lithosphere thickness using the thermal conductivity of the lherzolite, the previous calculation using pressure derivative of the thermal conductivity of 4% may cause an underestimation of the upper mantle lithosphere thickness by approximately 6% in a first approximation.

KEY WORDS: thermal diffusivity, lherzolite, pulse method, pressure derivative.

0 INTRODUCTION

Heat transfer inside the mantle is a key process controlling the Earth's dynamics. Lherzolite is the representative rock in subcontinental mantle lithosphere, and the study of its heat transfer properties will aid in understanding the thermal structure and rheological state of the upper mantle (Gong and Jiang, 2017; Zhou et al., 2015a; Wang and Cheng, 2012; Hofmeister, 1999). Although the heat transfer properties of olivine and pyroxene have received attention from the geophysics community, few studies have focused on heat transfer properties of lherzolite, especially at high pressure and high temperature (Hofmeister, 2012; Pertermann and Hofmeister, 2006; Osako et al., 2004; Xu et al., 2004; Katsura, 1995). Horai and Susaki (1989) applied the hot wire method to measure the thermal conductivity (k , $\text{Wm}^{-1}\text{K}^{-1}$) of lherzolite at pressure of 1.2 GPa and room temperature. Tommasi et al. (2001) applied a finite impulse heating method at ambient pressure and high temperature, and indicated that heat transport capability of the deformed upper mantle lherzolite being parallel to the flow direction is approximately 30% higher than that normal to the flow plane due to the lattice-preferred orientation. Gibert et al.

(2003a) adopted transient heating method to measure the thermal diffusivity (D , mm^2s^{-1} ; $k=D\rho C_P$, ρ is density, g/cm^3 ; C_P is heat capacity at constant pressure, $\text{J/(g}\cdot\text{K)}$) of lherzolite at ambient conditions. However, significant discrepancies remain with respect to the temperature dependence and absolute value of thermal diffusivity for lherzolite.

For most minerals, the pressure derivative of thermal conductivity (Hofmeister, 2007),

$$\partial(\ln k)/\partial P \cong \dot{K}/K_T \approx 4/K_T \quad (1)$$

where k is thermal conductivity, K_T is bulk modulus, \dot{K} is its pressure derivative, which is generally $\sim 4\%$ at room temperature (hereinafter, "pressure derivative of thermal conductivity" was called as " $d(\ln k)/dP$ " for short). For enstatite, $d(\ln k)/dP$ at room temperature is approximately 15.6% due to its relatively small K_T and large \dot{K} (Angel, 1994). One can expect that the thermal conductivity of lherzolite with a large quantity of enstatite may have a large $d(\ln k)/dP$ value. Gibert et al. (2003a) obtained $d(\ln k)/dP$ of approximately 12% for lherzolite at ambient temperature using finite impulse heating method. However, because the experimental pressure was relatively low (only 1 GPa), the obtained pressure dependence of thermal conductivity of the lherzolite was unconvincing. Moreover, $d(\ln k)/dP$ of minerals and rocks change with temperature, but there is little research on this subject, and this issue still remains poorly understood.

The present study used a pulse method to measure the thermal diffusivity of lherzolite at pressures ranging of 1.0–4.0

*Corresponding author: miaosheqiang@126.com

© China University of Geosciences (Wuhan) and Springer-Verlag GmbH Germany, Part of Springer Nature 2019

Manuscript received September 22, 2016.

Manuscript accepted April 24, 2017.

GPa and temperatures of 300–1 073 K and obtained $d(\ln k)/dP$ at different temperatures using the relational expression (Hofmeister, 2007).

$$\partial(\ln k)/\partial P \approx 1/K_T + \partial(\ln D)/\partial P \quad (2)$$

1 EXPERIMENTAL METHODS

1.1 Sample Preparation

The spinel lherzolite sample used in the experiment was collected from Damaping of Zhangjiakou, Hebei Province, which occurs as a xenolith in Cenozoic basalt. The inclusion studies indicated that it originated from approximately 42–60 km deep in the crust-mantle transition zone in which the temperature varies of 870–1 000 °C and the pressure is 1.4–2.0 GPa (Feng et al., 1982). The density of the samples was measured under ambient condition, according to Archimedes' principle, and the value is $3.26 \text{ g}\cdot\text{cm}^{-3}$. The porosity was measured using the Micro-ultra PYC 1200e true density analyzer, which was 1.6% for this sample.

Microscopic observations indicated that the sample was mainly composed of olivine and pyroxene, with a granular mosaic structure and an average particle size of 0.3 mm (Zhang et al. 2017). The sample contained 55% olivine (volumetric fraction, hereinafter), 22% orthopyroxene, 20% clinopyroxene, 3% spinel, and a little serpentine. The mineralogical composition was determined using thin sections and point-counting technique under a polarizing microscope.

The chemical compositions of the rock and its main minerals are shown in Table 1.

The samples were initially cut into three thick disks with a diameter of 10.00 mm. By thinning and polishing, the final samples have thickness of about 2.50 mm. They were dried at 323 K prior to the experiment, and then annealed at 473 K for 24 hours in an oven to remove the absorbed water from the sample.

1.2 Thermal Diffusivity Measurements

The thermal diffusivity of the samples was measured at high temperature and pressure on a YJ-3000t cubic press apparatus at IGCAS, Guiyang.

A schematic drawing of the sample assembly is shown in Fig. 1, which is similar to that of Osako et al. (2004). The sample consists of three identical disks stacked together. An impulse heater and a thermocouple were arranged between each two interfaces of disks, respectively (Kubičár et al., 2005). The diameter of the impulse heater was 10.00 mm folded from 0.127-mm-diameter NiCr wires. The temperature was measured using a NiCr-NiSi thermocouple with diameter of 0.127 mm (temperature deviation: $\pm 5 \text{ K}$). The magnesium oxide in contact with the sample has a relatively high thermal conductivity, which ensures that the excessive heat inside the sample can be rapidly released after each measurement session to achieve its own thermal equilibrium. The sample and heater were insulated with an alumina sample tube. In addition, a thermocouple wire and a heating

Table 1 Chemical compositions of the rock and its main constituent minerals (wt.%)

Oxides	SiO ₂	TiO ₂	Al ₂ O ₃	FeO*	MnO	CaO	Na ₂ O	K ₂ O	P ₂ O ₅	CO ₂	MgO	Cr ₂ O ₃	Total
Rock	46.00	0.05	2.43	7.36	0.15	2.56	0.24	0.01	0.02	4.10	36.43	-	99.35
OI	42.24	0.02	0.28	8.64	0.19	-	-	-	-	-	48.71	0.07	100.15
Cpx	53.35	0.81	5.16	4.36	0.09	21.6	1.74	-	-	-	13.18	0.58	100.87
Opx	54.88	-	3.58	10.99	0.06	0.51	0.04	0.04	-	-	29.69	0.22	100.01
Cr	-	-	23.46	24.55	-	0.04	-	-	-	-	9.95	40.06	98.06

Note: OI. Olivine; Cpx. clinopyroxene; Opx. orthopyroxene; Cr. chrome spinel; FeO*. whole iron; -, no detection. Analytical method for rock was X-ray fluorescence analysis, for minerals was electron microprobe analysis.

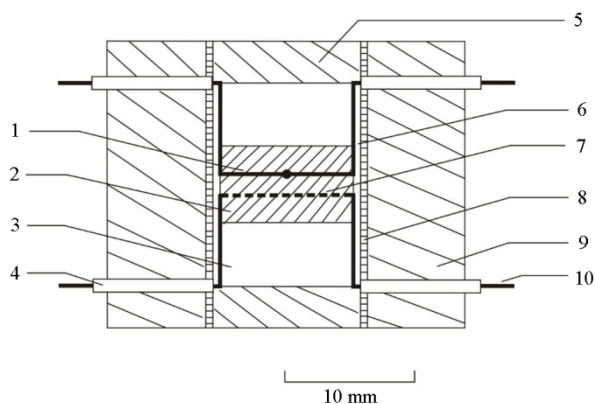


Figure 1. Schematic drawing of the sample assembly for measuring the thermal diffusivity at high temperature and pressure. 1. Thermocouple; 2. sample; 3. MgO block; 4. MgO sleeve; 5. Pyrophyllite space; 6. Al₂O₃ sample tube; 7. impulse heater; 8. heater; 9. pyrophyllite; 10. lead.

wire were both enclosed in the alumina ceramic tube, which had an inner diameter of 0.2 mm. The pyrophyllite cylinder, which served as the plug, and the cubic pyrophyllite, which served as the pressure medium (side length = 32.5 mm), were both heated to 1 073 K to prevent dehydration of the pyrophyllite at high temperature during the measurement (Xu et al., 2017).

During the experiment, we manually increased the pressure at a rate of 2.0 GPa/h to the desired pressure (error: $\pm 0.1 \text{ GPa}$); the temperature slowly increased automatically at a rate of 200 K/h until it reached the value required for measurement at constant pressure. A 100 K temperature interval was used for the continuously recorded data points. When the sample reached the target pressure and temperature conditions at which it became stable, a heating pulse of length $t_0=100 \text{ ms}$ was applied to the impulse heater through an integrated circuit and stabilized voltage supply controlled by an electronic switch. The samples on both sides of impulse heater were heated, and the heat was

transferred up- and downward. The heat transferred upward was detected by the thermocouple placed on top. The temperature signals processed by the potentiometer and DC amplifier were sent to the oscilloscope for display and collection.

The heat exchanged between the sample and environment can be ignored if the thickness of sample is small enough compared to its diameter and that the heat capacity and thickness of impulse heater were negligible, the heat transfer process above can be abstracted as a one-dimensional unsteady heat transfer of a semi-infinite object. The temperature response to the heat pulse at the thermocouple junction can be expressed as (Miao et al., 2014)

$$T(h, t) = \frac{q}{c_p \rho \sqrt{\pi D t}} \exp\left(-\frac{h^2}{4Dt}\right) \quad (3)$$

Here, h denotes the distance between heater and thermocouple, t is the time from the onset of heating, q is the heat flow across the section.

By taking the derivative of the right side of Eq. (3) and set it equal to 0. One can derive the equation

$$D = h^2 / 2t_m \times f_D \quad (4)$$

where f_D is the correction coefficient

$$f_D = \left(\frac{t_m}{t_0} - 1\right) \ln \left[\frac{t_m/t_0}{(t_m/t_0) - 1}\right], \text{ in the limiting case of } t_0 \rightarrow 0,$$

f_D has the value of 1). h is the sample thickness (mm), t_m represents the time(s) required for the thermocouple to reach the highest temperature response, and t_0 is the pulse time(s). According to the obtained curve, the time required for the thermocouple to reach the maximum temperature t_m was derived as presented in Fig. 2. The sample thickness h was introduced into Eq. (4) to derive the thermal diffusivity of the sample.

Errors are caused mainly by the uncertainty of sample thickness, and artificial error of judgment of the peak time. We estimate the total errors on the measurements to be less than 10%.

2 RESULTS AND DISCUSSIONS

In Fig. 3 the experimental results are presented and fitted

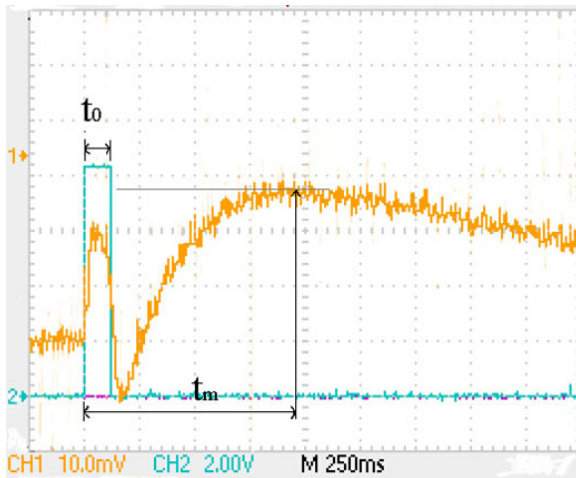


Figure 2. An input pulse and temperature response recorded using the oscilloscope (pulse length $t_0=120$ ms, $t_m=950$ ms. The horizontal scale interval time is 250 ms, the unit on the vertical is 10.0 mV for CH1 channel, 2.00 V for CH2 channel).

to the formula (Osako et al., 2004).

$$D = (a + b/T)(1 + cP) \quad (5)$$

The experimental results at high temperatures and high pressures were extrapolated to ambient temperature and pressure according to Eq. (5), yielding a thermal diffusivity for lherzolite of $2.10 \text{ mm}^2\text{s}^{-1}$, which is between the results of Horai and Susaki (1989) and Gibert et al. (2003a). The data of Horai and Susaki (1989) were extrapolated from high pressure to ambient pressure, and the data of Gibert et al. (2003a) represented the average of the data in the X and Z directions. The results at ambient pressure were below those of Gibert et al. (2013a), probably because the Alpine lherzolite used by Gibert contains more olivine than the lherzolite from North China used in this experiment. At moderate temperatures, these results were slightly below those of Gibert et al. (2005) for dunite, which can also be attributed to dunite's olivine content and high thermal diffusivity. At high temperatures, their experiments demonstrated considerable thermal radiation, resulting in an upward trend in the curve. The data was fitted to equation (Hofmeister, 2006).

$$D = a + b/T \quad (6)$$

The fitting coefficients are provided in Table 2.

Figure 4 shows the $d(\ln k)/dP$ for lherzolite as a function of temperature, which can be fitted as

$$\frac{d(\ln k)}{dP} = 0.13078 - 3.99067T.$$

As expected, $d(\ln k)/dP$ at ambient temperature obtained in this experiment was 12.1%, which is similar to the 11.9% obtained by Horai and Susaki (1989) and the 12.0% obtained by Gibert et al. (2003b). $d(\ln k)/dP$ gradually decreased with temperature, which is consistent with the experimental results of other studies. For example, Fujisawa et al.'s (1968) work on sterite yielded pressure coefficients of $17\% \text{ GPa}^{-1}$ at 700 K and $8\% \text{ GPa}^{-1}$ at 1100 K. Beck et al.'s (1978) work on dunite yielded $d(\ln k)/dP$ of $12.2\% \text{ GPa}^{-1}$ at 364 K and $7.1\% \text{ GPa}^{-1}$ at 515 K. For thermal conductivity of olivine aggregate, Katsura (1995) got $d(\ln k)/dP$ of 5.6% at 400 K,

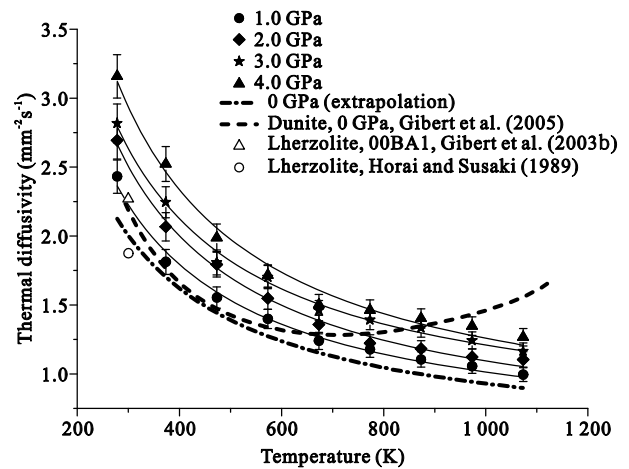
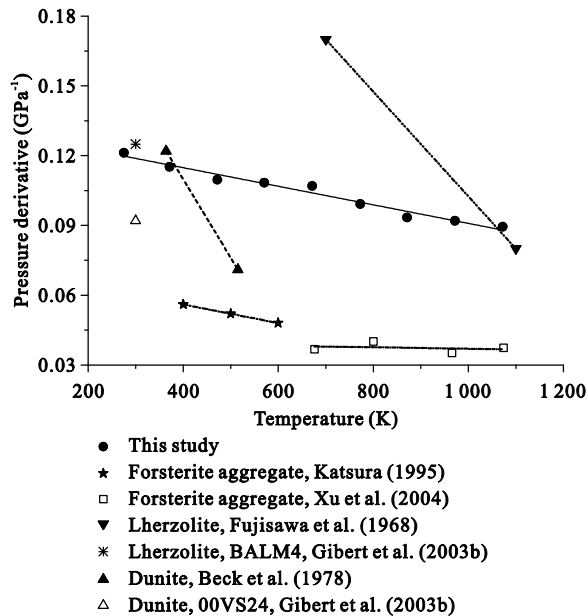


Figure 3. Thermal diffusivities of lherzolite at high pressures and high temperatures and comparison with previous works.

Table 2 Fitting coefficients for the thermal diffusivity to Eq. (6)

Pressure (GPa)	<i>a</i>	<i>b</i>	R ²
0	0.469 61	4.603 25×10 ²	0.999 89
1.0	0.493 45	5.199 24×10 ²	0.990 68
2.0	0.488 44	6.050 85×10 ²	0.995 27
3.0	0.597 98	6.107 06×10 ²	0.993 95
4.0	0.538 74	7.188 24×10 ²	0.987 39

**Figure 4.** $d(\ln k)/dP$ for lherzolite as a function of temperature (according to Eq. (2), K_T at high temperature was from Anderson et al. (1992))

5.2% at 500 K and 4.8% at 600 K. We attributed the high value of $d(\ln k)/dP$ for lherzolite to that of enstatite, this also can be confirmed from Fig. 4, in which lherzolite always shows high value of $d(\ln k)/dP$ than that of dunite and forsterite aggregate (Xu et al., 2004).

$d(\ln k)/dP$ of lherzolite obtained in this experiment was approximately 10% at 1 073 K, which is higher than the previously determined value of 4% in the same conditions. Therefore, at high pressure, the thermal conductivity of the mantle lithosphere is greater, and the temperature gradient of the mantle lithosphere is smaller than previously thought. In calculating the lithosphere thickness, the quantity of heat generated by the upper mantle is small enough to be considered negligible; therefore, the heat conduction in the upper mantle lithosphere can be simplified to a one-dimensional steady-state planar heat conduction problem (Xu et al. 2017). According to the Fourier's thermal conduction equation: $q = k\Delta T/\Delta z$, in which q is surface heat flow, ΔT is a constant, the thermal conductivity k is proportional to the lithosphere thickness, Δz (Zhou et al. 2015b). Therefore, the results calculated using $d(\ln k)/dP$ for the lithospheric mantle of 4% rather than 10%, may underestimate the thickness of the upper mantle lithosphere by 6% in a first approximation.

3 CONCLUSIONS

This study utilized a pulse method to measure the thermal

diffusivity of lherzolite at pressures of 1.0–4.0 GPa and temperatures of 300–1 073 K on a cubic press apparatus. We obtained a thermal diffusivity for lherzolite of approximately $2.10 \text{ mm}^2\text{s}^{-1}$ at ambient condition, which is consistent with the experimental results of other studies. We found that the experimental $d(\ln k)/dP$ of lherzolite decreased with temperature decline, reaching approximately 10% at high temperature, which is higher than the previous experimental data, which indicates that the temperature gradient of the upper mantle lithosphere is smaller than previous thought. Therefore, in calculating the lithosphere thickness using the thermal conductivity of the lherzolite, the previous calculation used $d(\ln k)/dP$ of 4% may cause an underestimation of the upper mantle lithosphere thickness by approximately 6% in a first approximation.

ACKNOWLEDGMENTS

This study was sponsored by the National Natural Science Foundation of China (No. 41504072), the “135” Program of Institute of Geochemistry, Chinese Academy of Sciences (CAS) and State Key Laboratory of Earthquake Dynamics (No. LED2015A04). Two anonymous reviewers are greatly appreciated for improving the manuscript. The final publication is available at Springer via <https://doi.org/10.1007/s12583-018-0868-3>.

REFERENCES CITED

- Anderson, O. L., Isaak, D., Oda, H., 1992. High-Temperature Elastic Constant Data on Minerals Relevant to Geophysics. *Reviews of Geophysics*, 30(1): 57–90. <https://doi.org/10.1029/91rg02810>
- Angel, R. J., 1994. Feldspars at High Pressure. In: Parsons, L., ed., *Feldspars and Their Reactions*. Springer, Netherlands. 271–312
- Beck, A. E., Darbha, D. M., Schloessin, H. H., 1978. Lattice Conductivities of Single-Crystal and Polycrystalline Materials at Mantle Pressures and Temperatures. *Physics of the Earth and Planetary Interiors*, 17(1): 35–53. [https://doi.org/10.1016/0031-9201\(78\)90008-0](https://doi.org/10.1016/0031-9201(78)90008-0)
- Feng, J., Xie, M., Zhang, H., et al., 1982. Hannuoba Basalts and Nodules Derived from the Deep Earth. *Bulletin of Hebei College of Geology*, 1: 45–63
- Fujisawa, H., Fujii, N., Mizutani, H., et al., 1968. Thermal Diffusivity of Mg_2SiO_4 , Fe_2SiO_4 , and NaCl at High Pressures and Temperatures. *Journal of Geophysical Research*, 73(14): 4727–4733. <https://doi.org/10.1029/jb073i014p04727>
- Gibert, B., Schilling, F. R., Tommasi, A., et al., 2003a. Thermal Diffusivity of Olivine Single-Crystals and Polycrystalline Aggregates at Ambient Conditions—A Comparison. *Geophysical Research Letters*, 30(22): 2172–2176. <https://doi.org/10.1029/2003gl018459>
- Gibert, B., Seipold, U., Tommasi, A., et al., 2003b. Thermal Diffusivity of Upper Mantle Rocks: Influence of Temperature, Pressure, and the Deformation Fabric. *Journal of Geophysical Research*, 108(B8): 1–15. <https://doi.org/10.1029/2002jb002108>
- Gibert, B., Schilling, F. R., Gratz, K., et al., 2005. Thermal Diffusivity of Olivine Single Crystals and a Dunite at High Temperature: Evidence for Heat Transfer by Radiation in the Upper Mantle. *Physics of the Earth and Planetary Interiors*, 151(1/2): 129–141. <https://doi.org/10.1016/j.pepi.2005.02.003>
- Gong, W., Jiang X. D. 2017. Thermal Evolution History and Its Genesis of the Ailao Shan-Red River Fault Zone in the Ailao Shan and Day Nui Con Voi Massif during Oligocene–Early Miocene. *Earth*

- Science—Journal of China University of Geosciences*, 42(2): 223–239 (in Chinese with English Abstract)
- Hofmeister, A. M., 1999. Mantle Values of Thermal Conductivity and the Geotherm from Phonon Lifetimes. *Science*, 283(5408): 1699–1706. <https://doi.org/10.1126/science.283.5408.1699>
- Hofmeister, A. M., 2006. Thermal Diffusivity of Garnets at High Temperature. *Physics and Chemistry of Minerals*, 33(1): 45–62. <https://doi.org/10.1007/s00269-005-0056-8>
- Hofmeister, A. M., 2007. Pressure Dependence of Thermal Transport Properties. *Proceedings of the National Academy of Sciences of the United States of America*, 104(22): 9192–9197
- Hofmeister, A. M., 2012. Thermal Diffusivity of Orthopyroxenes and Protoenstatite as a Function of Temperature and Chemical Composition. *European Journal of Mineralogy*, 24(4): 669–681. <https://doi.org/10.1127/0935-1221/2012/0024-2204>
- Horai, K. I., Susaki, J. I., 1989. The Effect of Pressure on the Thermal Conductivity of Silicate Rocks up to 12 kbar. *Physics of the Earth and Planetary Interiors*, 55(3/4): 292–305. [https://doi.org/10.1016/0031-9201\(89\)90077-0](https://doi.org/10.1016/0031-9201(89)90077-0)
- Katsura, T., 1995. Thermal Diffusivity of Olivine under Upper Mantle Conditions. *Geophysical Journal International*, 122(1): 63–69. <https://doi.org/10.1111/j.1365-246x.1995.tb03536.x>
- Kubičár, E., Vretenár, V., Hammerschmidt, U., 2005. Thermophysical Parameters of Optical Glass BK 7 Measured by the Pulse Transient Method. *International Journal of Thermophysics*, 26(2): 507–518. <https://doi.org/10.1007/s10765-005-4512-y>
- Miao, S. Q., Li, H. P., Chen, G., 2014. Measurement of Thermal Diffusivity for Rocks at High Temperature and High Pressure—Application to Basalt. *Chinese Journal of High Pressure Physics*, 28: 11–17 (in Chinese with English Abstract)
- Osako, M., Ito, E., Yoneda, A., 2004. Simultaneous Measurements of Thermal Conductivity and Thermal Diffusivity for Garnet and Olivine under High Pressure. *Physics of the Earth and Planetary Interiors*, 143-144: 311–320. <https://doi.org/10.1016/j.pepi.2003.10.010>
- Pertermann, M., Hofmeister, A. M., 2006. Thermal Diffusivity of Olivine-Group Minerals at High Temperature. *American Mineralogist*, 91(11/12): 1747–1760. <https://doi.org/10.2138/am.2006.2105>
- Tommasi, A., Gibert, B., Seipold, U., et al., 2001. Anisotropy of Thermal Diffusivity in the Upper Mantle. *Nature*, 411(6839): 783–786. <https://doi.org/10.1038/35081046>
- Wang, Y., Cheng, S. H., 2012. Lithospheric Thermal Structure and Rheology of the Eastern China. *Journal of Asian Earth Sciences*, 47: 51–63. <https://doi.org/10.1016/j.jseaes.2011.11.022>
- Xu, L. L., Jin, Z. M., Mei, S. H., 2017. Deformation-DIA Coupled with Synchrotron X-Ray Diffraction and Its Applications to Deformation Experiments of Minerals at High Temperature and High Pressure. *Earth Science—Journal of China University of Geosciences*, 42(6): 974–989 (in Chinese with English Abstract)
- Xu, Y. S., Shankland, T. J., Linhardt, S., et al., 2004. Thermal Diffusivity and Conductivity of Olivine, Wadsleyite and Ringwoodite to 20 GPa and 1373 K. *Physics of the Earth and Planetary Interiors*, 143/144: 321–336. <https://doi.org/10.1016/j.pepi.2004.03.005>
- Xu, Y. X., Zhu, L. P., Wang, Q. Y., et al., 2017. Heat Shielding Effects in the Earth's Crust. *Journal of Earth Science*, 28(1): 161–167. <https://doi.org/10.1007/s12583-017-0744-6>
- Zhang, Y. F., Hu, C. L., Wang, X. M., et al., 2017. An Improved Method of Laser Particle Size Analysis and Its Applications in Identification of Lacustrine Tempestite and Beach Bar: An Example from the Dongying Depression. *Journal of Earth Science*, 28(6): 1145–1152. <https://doi.org/10.1007/s12583-016-0930-1>
- Zhou, F. Z., Zheng, X. H., 2015a. Heat Transfer in Tubing-Casing Annulus during Production Process of Geothermal Systems. *Journal of Earth Science*, 26(1): 116–123. <https://doi.org/10.1007/s12583-015-0511-5>
- Zhou, F. Z., Xiong, Y. C., Tian, M., 2015b. Predicting Initial Formation Temperature for Deep Well Engineering with a New Method. *Journal of Earth Science*, 26(1): 108–115. <https://doi.org/10.1007/s12583-015-0512-4>